Orientational Ordering and Dynamics in the Columnar Phase of a Discotic Liquid Crystal Studied by Deuteron NMR Spectroscopy

ARTICLE *in* THE JOURNAL OF CHEMICAL PHYSICS · MARCH 1998

Impact Factor: 2.95 · DOI: 10.1063/1.475833

6 AUTHORS, INCLUDING:

Ronald Y Dong
University of British Columbia - Vancouver
219 PUBLICATIONS **2,261** CITATIONS
SEE PROFILE

Neville Boden
University of Leeds
87 PUBLICATIONS **3,131** CITATIONS
SEE PROFILE

Orientational ordering and dynamics in the columnar phase of a discotic liquid crystal studied by deuteron NMR spectroscopy

X. Shen
Physics Department, University of Manitoba, Winnipeg Manitoba, R3T 2N2, Canada

Ronald Y. Dong[a)]
Department of Physics and Astronomy, Brandon University, Brandon, Manitoba, R7A 6A9, Canada

N. Boden, R. J. Bushby, P. S. Martin, and A. Wood
Centre for Self-Organising Molecular Systems, The University of Leeds, Leeds, LS2 9JT, United Kingdom

(Received 22 October 1997; accepted 4 December 1997)

We report on a deuteron NMR study of quadrupolar splittings and spin-lattice relaxation times T_{1Q} and T_{1Z} as a function of temperature and at two different Larmor frequencies in the columnar phase of hexakis(*n*-hexyloxy)triphenylene (HAT6). The additive potential method is used to model the quadrupolar splittings, from which the potential of mean torque is parameterized, and the order parameter tensor for an ''average'' conformer is determined. The small-step rotational diffusion model is used to find the rotational diffusion constants $D_{\parallel}$ and $D_{\perp}$ for the spinning and tumbling motions of the molecular core. It is found that $D_{\perp}$ is slightly larger than $D_{\parallel}$ in contrast with the findings in calamitic liquid crystals. The decoupled model of Dong for correlated internal rotations in the end chains is used for the first time in a discotic liquid crystal. Both jump constants for one- and three-bond motions are nearly independent of temperature, while the jump constant for two-bond motion is thermally activated. The rotational speeds $D_{\parallel}$ and $D_{\perp}$ are some two orders of magnitude slower than a typical charge hopping frequency between the aromatic cores of adjacent molecules in the columns. Thus, to a migrating charge, the ''lattice'' appears static with disorder being due to the instantaneous displacement of the cores with respect to each other. © *1998 American Institute of Physics.* [S0021-9606(98)51210-X]

INTRODUCTION

The novel charge transport properties of the columnar phases[1] formed by disk-like molecules such as the hexakis-(alkyloxy)triphenylenes (HAT*n*) are potentially exploitable in applications ranging from sensing devices to high-resolution xerography.[2] These disk-like molecules are stacked, with only short-range positional order, into columns which are arranged on a two-dimensional lattice, typically hexagonal (Figure 1). The fluctuations in columnar orders are sufficient to suppress inhomogeneously distributed structural traps and give rise instead to a uniform ''liquid-like'' dynamic disorder. A consequence of this is that the individual molecular columns can transport electronic charge with well defined Gaussian transits.[3–5] Charge carrier mobilities along the columns $\mu_{\parallel}$ can be as high as 10^{-2} cm^2 V^{-1} s^{-1} and are typically 10^3 quicker than in the perpendicular direction.[6] In HAT6, $\mu_{\parallel}$ is about 10^{-4} cm^2 V^{-1} s^{-1} and the intra- and inter-columnar distances are $d_{\parallel} \simeq 3.5$ Å and $d_{\perp} \simeq 19.5$ Å, so that using $\mu = eD^t/k_BT$ we calculate the translational diffusion constants $D^t_{\parallel} = 5 \times 10^{-6}$ cm^2/s and $D^t_{\perp} = 5 \times 10^{-9}$ cm^2/s for ionic diffusivity. The latter is two orders of magnitude smaller than the value of 5×10^{-7} cm^2/s measured by NMR[7] for the molecular self-diffusion constant perpendicular to the columnar axis. Thus, the charge carrier, a positive hole, is carried from column-to-column by the molecular hop. The transport of charges along the column is dependent on the overlap of π-orbitals between adjacent aromatic rings, which is very sensitive to the distance of closest approach and the relative reorientation of the rings and their time dependence. It is, therefore, important to have a detailed description of the molecular reorientational motion within the columns.

It is well known[8] that deuterium NMR spectroscopy can provide detailed information on the orientational ordering and dynamics in mesophases of liquid crystals. In particular, one can rely on theoretical models to extract relevant motional parameters from deuteron spin-lattice relaxation times. The small-step rotational diffusion model[9,10] has been successfully used in liquid crystals to describe symmetric-top molecules reorienting in a potential of mean torque set up by their neighbors. Deuterated HAT*n* molecules have been studied using proton and deuteron NMR by Luz and co-workers[7,11–13] more than 10 years ago. To explain[14] the spectral densities of aromatic deuterons in HAT6, the Nordio model[9] was used and rotational diffusion constants for the HAT6 molecule were derived. The quadrupolar splittings of the chain deuterons were modeled[15] using the so-called additive potential (AP) method which was pioneered by Marcelja[16] and extended subsequently by Emsley, Luckhurst, and Stockley.[17] This earlier attempt for the homologous series HAT*n* unfortunately contained numerical errors and the good fits were therefore fortuitive. In the present study, the quadrupolar splittings are used to obtain[8] the order param-

[a)]Author to whom correspondence should be addressed.

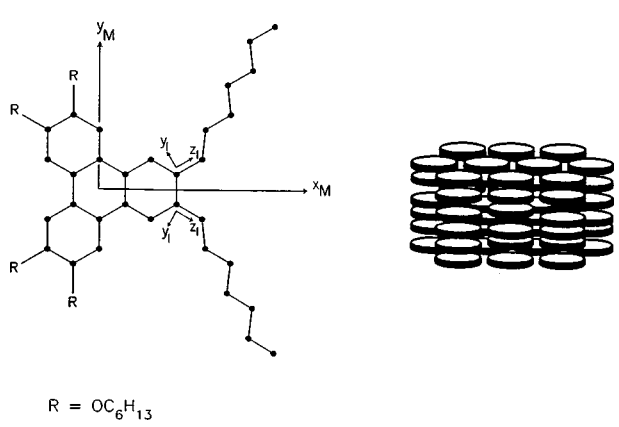

FIG. 1. Hexakis(n-hexyloxy)triphenylene (HAT6) shown with coordinate systems used in the text, and a schematic view of its columnar D_h mesophase.

eters $\langle P_2 \rangle$ and $\langle S_{xx}-S_{yy} \rangle$ for an ''average'' conformer. These in turn determine at each temperature the orienting potential (a_{20}, a_{22})[10] needed for solving the rotational diffusion equation. The decoupled model[18] is used to deal with the dynamics of internal bond rotations. In this model, internal rotations in a flexible chain are assumed to obey a master equation and are decoupled from the overall reorientation of the molecule. A realistic geometry is used for HAT6 to generate all possible conformations in one of the chains using the Flory model.[19] Since the $O-C_1$ bond is taken[12] to be on the plane of the aromatic core, there are 243 conformations in the chain. The transition rate matrix R, which describes conformational changes in the chain, is a 243×243 matrix and contains jump constants[18] k_1, k_2, and k_3 for the one-, two- and three-bond motions in the chain. We use a global target approach[20] to analyze all the spectral density data at different temperatures and frequencies in the same fitting procedure. This has been found to give reliable target model parameters in calamitic liquid crystals. The paper is organized as follows. A theory section outlines the required formulae used to analyze the quadrupolar splittings and spectral density data. This is followed by an experimental section on the synthesis of deuterated HAT6 samples and on the NMR method. The last section is on results and discussion.

THEORY

The constituent molecules of liquid crystals (e.g., MBBA, HAT6) usually contain an aromatic core and one or more flexible side chains. NMR studies[8] of order parameter profiles in these molecules have revealed that the ordering of their rigid segments varies with respect to each other and with temperature. The AP method of getting a potential of mean torque for flexible molecules is outlined first. Marcelja[16] was the first to explicitly consider the alkyl chain in calculating physical properties of liquid crystals. The rotational isomeric state model[19] is used to determine all of the allowed conformations. Each molecular conformer is assumed as a perfectly rigid entity. In this model, the bond lengths are taken to be fixed. Rotation about each carbon–carbon (C–C) bond in the chain may take one of the three dihedral angles ($\phi=0, \pm112°$). These ϕ angles correspond to the *trans* (t) and two symmetric *gauche* ($g^{\pm}$) states. The *gauche* states have higher energy in comparison to that of the *trans* by an amount E_{tg}. The potential energy $U(j,\Omega)$ of a molecule in a conformation j and a particular orientation Ω with respect to the director is given by

$$U(j,\Omega)=U_{int}(j)+U_{ext}(j,\Omega), \tag{1}$$

where the potential of mean torque $U_{ext}(j,\Omega)$ originates from the molecular field of its neighbors, and $U_{int}(j)$, the internal energy, is assumed to depend on the number (N_g) and not the location of the *gauche* linkages in the chain, as well as $N_{g\pm g\mp}$, the number of g^+g^- or g^-g^+ linkages in the chain

$$U_{int}(j)=N_gE_{tg}+N_{g\pm g\mp}E_{g\pm g\mp}. \tag{2}$$

These g^+g^- or g^-g^+ linkages have higher internal energy $E_{g\pm g\mp}$ because they bring parts of the chain near to one another, the so-called ''pentane effect.'' The potential of mean torque depends on the polar angles of the director in a molecular frame that is attached to a particular rigid segment of the molecule. In the AP method, it is assumed that the molecule can be divided into a small number of rigid segments. Each segment is associated with an interaction tensor that is independent of the conformation. The total interaction tensor of a particular conformer is calculated by transforming the tensors from their segmental axis systems into a common system and then adding them together to give $U_{ext}(j,\Omega)$. The location of this common molecular frame is not critical, and a convenient choice is a frame set on the aromatic core of the molecule.

In a deuterium NMR experiment, one obtains quadrupolar splittings for the methylene deuteron(s) ($\eta=0$) at the ith site:

$$\begin{aligned}\Delta\nu_i&=\frac{3}{2}q_{CD}^{(i)}P_2(\cos\Theta)\sum_n p_nS_{bb}^{n,i}\\&=\frac{3}{2}q_{CD}^{(i)}P_2(\cos\Theta)S_{CD}^{(i)},\end{aligned} \tag{3}$$

where $q_{CD}^{(i)}=(e^2qQ/h)_i$ is the quadrupolar coupling constant, $P_2(x)=(3x^2-1)/2$, Θ is the angle between the director and the external magnetic field, and $S_{CD}^{(i)}$ is a weighted average of the segmental order parameter $S_{bb}^{n,i}$ for the $C_i-{}^2H$ bond of the molecule with conformation n. Now p_n, the probability of finding the molecule with conformation n in a mesophase, is given by

$$p_n=\frac{1}{Z}\exp[-U_{int}(n)/k_BT]Q_n, \tag{4}$$

where Q_n, the orientational partition function of conformation n, is

$$Q_n=\int \exp[-U_{ext}(n,\Omega)/k_BT]d\Omega \tag{5}$$

and Z, the conformation-orientational partition function, is

$$Z=\sum_n \exp[-U_{int}(n)/k_BT]Q_n. \tag{6}$$

In writing down Eq. (3), one sets the principal axis frame (a,b,c) for the quadrupolar interaction with the b axis in the direction of the C_i-^2H bond. For the aromatic deuterons $(i=0)$, a η value of 0.064 is assumed, and their splitting is given by

$$\Delta\nu_0=\frac{3}{2}q_{CD}^{(0)}P_2(\cos\Theta)\sum_n p_n\left[S_{bb}^{n,0}+\frac{\eta}{3}(S_{aa}^{n,0}-S_{cc}^{n,0})\right]. \tag{7}$$

Now the order parameter for a particular direction k in the conformer n may be evaluated in the principal (x,y,z) frame of $U_{ext}(n,\Omega)$

$$S_{kk}^{n,i}=\sum_{\alpha}^{x,y,z} S_{\alpha\alpha}^{n}\cos^2\theta_{\alpha k}^{n,i}, \tag{8}$$

where $S_{\alpha\alpha}^{n}$, the principal components of the order matrix for the conformer n, may be written as

$$\begin{aligned} S_{xx}^{n}&=\frac{1}{2}(\sqrt{6}\langle d_{0,2}^2\cos 2\psi\rangle_n-\langle d_{0,0}^2\rangle_n),\\ S_{yy}^{n}&=-\frac{1}{2}(\sqrt{6}\langle d_{0,2}^2\cos 2\psi\rangle_n+\langle d_{0,0}^2\rangle_n),\\ S_{zz}^{n}&=\langle d_{0,0}^2\rangle_n, \end{aligned} \tag{9}$$

and $\theta_{\alpha k}^{n,i}$ denote angles for the C_i-^2H bond between the $k(=a,b,c)$ axis and a principal axis $\alpha(=x,y,z)$. The constructed interaction tensor $U_{ext}(n,\Omega)$ is first diagonalized to obtain the the interaction tensor components $X_{2,0}^n$ and $X_{2,\pm 2}^n$ for the conformer n. In the principal frame,

$$U_{ext}(n,\Omega)=-[X_{2,0}^n d_{0,0}^2(\theta)+2X_{2,2}^n d_{0,2}^2(\theta)\cos 2\psi] \tag{10}$$

and $\langle d_{0,0}^2\rangle_n$ and $\langle d_{0,2}^2\cos 2\psi\rangle_n$ can easily be obtained.[21]

To construct $U_{ext}(j,\Omega)$ for the conformer j, one needs to know the geometry of the chain. The CCC, CCH, and HCH angles are assumed[22] to be 113.5°, 107.5°, and 113.6°, respectively. For the alkyloxy chain, the O–C bond is taken to be identical to a C–C bond. However, the COC angle[23] and OCC angle are set at 126.4°, and the internal energies E_{tg}' and $E_{g^{\pm}g^{\mp}}'$ are used due to the presence of the oxygen. Suppose that the aromatic core has an interaction tensor $\epsilon_{\alpha\beta}^{(a)}$ and each C–C segment has an interaction tensor $\epsilon_{\alpha\beta}^{(c)}$. To write down these interaction tensors, care is needed to distinguish between calamitic and discotic mesogens. If these local interaction tensors are assumed to have cylindrical symmetry, then the interaction tensor $\epsilon_{\alpha\beta}^{(a)}$ for the disk-shaped core can be written as

$$X_a\begin{pmatrix} -\frac{1}{2} & 0 & 0\\ 0 & -\frac{1}{2} & 0\\ 0 & 0 & 1\end{pmatrix}$$

and the interaction tensor $\epsilon_{\alpha\beta}^{(c)}$ for the rodlike C–C segment is now given by

$$X_{cc}\begin{pmatrix} \frac{1}{4} & 0 & 0\\ 0 & \frac{1}{4} & 0\\ 0 & 0 & -\frac{1}{2}\end{pmatrix},$$

where X_a and X_{cc} are the core and C–C interaction parameters, respectively. In a local (1, 2, 3) frame where the 3 axis is along the C_j-C_{j+1} bond, the 1 axis is in the plane bisecting the HCH angle, and the 2 axis is chosen to complete a right-handed Cartesian coordinate system, the $C-^2H$ vector is given by

$$\mathbf{V}_{CD}=\begin{pmatrix} a\\ b\\ c\end{pmatrix}, \tag{11}$$

where $b=\sin(\angle HCH/2)$, $c=\cos(\angle CCH)$, and $a^2=1-b^2-c^2$. A common molecular frame is picked with the z_M axis perpendicular to the core plane (see Figure 1), and the x_M axis on the plane bisecting two of the six pendent chains. Here we construct the total interaction tensor for HAT6 by explicitly considering two chains as shown. All the $O-C_1$ bonds are on the x_My_M plane. The $C_{ar}-O$ bonds are included in the core when writing down the $\epsilon_{\alpha\beta}^{(a)}$; also included are the remaining four pendent chains. Furthermore, the conformations of the two chosen chains are assumed to be identical and non-interacting. These drastic assumptions are necessary to make the problem tractable. The orientation of the C_j-^2H vector in this frame is given by $\mathbf{V}_{CD}^M$,

$$\mathbf{V}_{CD}^M=R_{M,1}R_{1,2}\cdots_{j-1,j}\mathbf{V}_{CD}, \tag{12}$$

where $R_{j-1,j}$ is a rotation matrix that transforms between the jth local frame and the $(j-1)$th local frame. The $\mathbf{V}_{CD}^M$ for the aromatic deuteron can easily be found for one of the six deuterons in the core. To obtain the direction cosine in Eq. (8), it is necessary to get the C_j-^2H vector in the principal frame of the total interaction tensor,

$$\mathbf{V}_{CD}^p=R_{p,M}\mathbf{V}_{CD}^M, \tag{13}$$

where the rotation matrix $R_{p,M}$ contains the eigenvectors $(\mathbf{r}_i)$ obtained in diagonalizing the total interaction tensor $\epsilon_{\alpha,\beta}^n$ for each conformer. Now $\epsilon_{\alpha\beta}^n$ is obtained by

$$\epsilon_{\alpha\beta}^n=\epsilon_{\alpha\beta}^{(a)}+R_{M,1}\lambda_{\alpha\beta}^n R_{M,1}^{-1}+R_{M,1}'\lambda_{\alpha\beta}^n R_{M,1}'^{-1}, \tag{14}$$

where

$$\lambda_{\alpha\beta}^n=\sum_{j=2}^{7} R_{1,2}\cdots R_{j-1,j}\epsilon_{\alpha\beta}^{(c)}R_{j-1,j}^{-1}\cdots R_{1,2}^{-1} \tag{15}$$

and $R_{M,1}$ and $R_{M,1}'$ are rotation matrices for the two chains which transform between the first local frames to the molecular frame. We use Eq. (4) and Eqs. (8)–(10) to evaluate $\Delta\nu_i$ or $S_{CD}^{(i)}$ [Eqs. (3) and (7)]. For flexible molecules whose p_n and $S_{\alpha\beta}^n$ are known, it is possible to find a single conformationally averaged ordering matrix in a common molecular frame and then to find its diagonal elements for the ''averaged'' conformer[17,24] in a mesophase.

The Tarroni–Zannoni (TZ) model[10] is briefly surveyed in order to write down the spectral densities $J_m(m\omega)$ due to the core dynamics of HAT6. To evaluate the orientational

correlation functions for the molecular core, one needs to find the conditional probability by solving the rotational diffusion equation

$$\frac{1}{\rho}\frac{\partial \hat{P}(\Omega_0|\Omega t)}{\partial t}=\hat{\Gamma}\hat{P}(\Omega_0|\Omega t), \tag{16}$$

where the symmetrized diffusion operator $\hat{\Gamma}$ is given by Eq. (14) of Ref. 10. The rotational diffusion tensor in the molecular frame contains principal diffusion elements $D_x \equiv D_{xx}$, $D_y \equiv D_{yy}$ and $D_z \equiv D_{zz}$. Now $\hat{\Gamma}$ is written in terms of $\rho=(D_x+D_y)/2$, $\epsilon=(D_x-D_y)/(D_x+D_y)$, and $\eta=D_z/\rho$. For HAT6, the asymmetry parameter for rotational diffusion ϵ is zero. Therefore, the TZ model reduces to the Nordio model[9] (which has $D_x=D_y\equiv D_\perp$, $D_z\equiv D_\parallel$, and $a_{22}=0$). In general, the orientational correlation functions can be written as a sum of decaying exponentials[9,10]

$$g^2_{mnn'}(t)=\sum_K (\beta^2_{mnn'})_K \exp[(\alpha^2_{mnn'})_K t], \tag{17}$$

where $(\alpha^2_{mnn'})_K/\rho$, the decay constants, are the eigenvalues and $(\beta^2_{mnn'})_K$, the relative weights of the exponentials, are the corresponding eigenvectors from diagonalizing the $\hat{\Gamma}$ matrix whose elements are formed using a Wigner basis set. The solutions of the rotational diffusion equation involve ranks (L) up to 40 in the basis set, since the order parameter $\langle P_2\rangle$ of HAT6 is rather high. In the above equation, the projection indices (n,n') in the molecular frame are equal due to uniaxial symmetry of the HAT6 molecule.

We first consider spectral densities for the case where the director is along the magnetic field. The spectral densities for the ring (C_0) deuterons of HAT6 arise from molecular reorientations and are given by

$$J^{(0)}_m(m\omega)=\frac{3\pi^2}{2}(q^{(0)}_{CD})^2\sum_n [d^2_{n0}(\beta_{M,Q})]^2 \times\sum_K \frac{(\beta^2_{mnn})_K(\alpha^2_{mnn})_K}{(\alpha^2_{mnn})^2_K+m^2\omega^2}, \tag{18}$$

where the $\beta_{M,Q}$ angle between the C–^{2}H bond and the molecular z_M axis is taken to be 90°. In the decoupled model, the spectral densities $J^{(i)}_m(m\omega)$ of the C_i methylene deuteron(s) are given by[8]

$$\begin{aligned}J^{(i)}_m(m\omega)=&\frac{3\pi^2}{2}(q^{(i)}_{CD})^2\sum_n\sum_{j=1}^{N}|\sum_{l=1}^{N} d^2_{n0}(\beta^{(i)l}_{M,Q})\\ &\times\exp[-in\alpha^{(i)l}_{M,Q}]x^{(1)}_l x^{(j)}_l|^2\\ &\times\sum_K\frac{(\beta^2_{mnn})_K[(\alpha^2_{mnn})_K+|\wedge_j|]}{[(\alpha^2_{mnn})_K+|\wedge_j|]^2+m^2\omega^2}\\ &+\frac{3\pi^2}{2}(q^{(i)}_{CD})^2\delta_{m0}\langle P_2\rangle^2\\ &\times\sum_{j=1}^{N}|\sum_{l=1}^{N} d^2_{00}(\beta^{(i)l}_{M,Q})x^{(1)}_l x^{(j)}_l|^2/|\wedge_j|,\end{aligned} \tag{19}$$

where $N=243$, $q^{(i)}_{CD}=165$ kHz, $\beta^{(i)l}_{M,Q}$ and $\alpha^{(i)l}_{M,Q}$ are the polar angles of the C_i–^{2}H bond of the conformer l in the molecular M frame. $\wedge_j$ and $\mathbf{x}^{(j)}$ are the eigenvalues and eigenvectors from diagonalizing a symmetrized transition rate matrix $\underline{\underline{R}}$. The last term in the above equation is due to a cross-term contribution between internal bond rotations and the molecular reorientation.

Since HAT6 has $\Delta\chi<0$, the columnar axes (directors) are aligned perpendicular to the magnetic field. The measured T_{1Z} and T_{1Q} give $J_1(\omega,90°)$ and $J_2(2\omega,90°)$. These can be calculated in terms of $J_m(m\omega,0°)\equiv J_m(m\omega)$ $(m=0,1,2)$ as follows:[8]

$$J^{(i)calc}_1(\omega,90°)=\frac{1}{2}[J^{(i)}_1(\omega)+J^{(i)}_2(\omega)], \tag{20}$$

$$J^{(i)calc}_2(2\omega,90°)=\frac{3}{8}J^{(i)}_0(2\omega)+\frac{1}{2}J^{(i)}_1(2\omega)+\frac{1}{8}J^{(i)}_2(2\omega). \tag{21}$$

Substituting Eqs. (18) and (19) into the above equations, the measured spectral densities in our experiments can be calculated.

EXPERIMENTAL METHOD

Synthesis: 2,3-(d_{13})Hexyloxy-6,7,10,11-tetrahexyloxytriphenylene

Perdeuterated 1-bromohexane **2**

Perdeuterated hexan-1-ol (500 mg; 4.3 mmol) **1** was added drop wise to a vigorously stirred solution of hydrobromic acid (2.49 g; 48% w/v) and concentrated sulphuric acid (426 mg). The mixture was refluxed for 6 h, cooled and carefully poured onto water (50 ml). The aqueous mixture was extracted with diethylether (2×50 ml), and washed consecutively with sodium hydrogen carbonate solution (50 ml), water (50 ml) and again sodium hydrogen carbonate solution (50 ml) the organic layer being dried over anhydrous magnesium sulphate. Filtration, and solvent evaporation at RT yielded deuterated 1-bromo-hexane (660 mg; 85%) **2** as a dark brown liquid which was used in its crude state for the next step.

1,2-Dihexyloxy-4-iodobenzene **3**

Iodine monochloride (60 g) was slowly added to a vigorously stirred solution of 1,2-dihexyloxy benzene (72.5 g; 0.216 mol) in chloroform (200 ml) at 0 °C. After stirring at room temperature for 1 h the solution was decanted and washed with aqueous sodium metabisulfite. Evaporation of the organic layer produced a crude product which was distilled under reduced pressure to give 1,2-dihexyloxy-4-iodobenzene **3** (69.1 g, 79%) as a dark brown oil (bp 240–260 °C at 40 mmHg).[24] ^{1}H NMR ($CDCl_3$) δ: 7.09 (s, 1H, ArH), 7.05 (d, 1H, J= 8.5 Hz, ArH), 6.50 (d, 1H, J=8.5 Hz, ArH), 3.97 (t, 4H, J=7 Hz, OCH_2), 1.81 (m, 4H, J=7 Hz, OCH_2CH_2), 1.33–1.49 (m, 12H, CH_2). 0.97 (t, 6H, J=7 Hz, CH_3).

3,3′,4,4′-Tetrahexyloxybiphenyl 4

1,2-Dihexyloxy-4-iodobenzene (16 g; 0.04 mol) **3** was intimately mixed with copper powder (30 g) and heated carefully to 270 °C where an exothermic reaction took place causing the temperature to rise to 310 °C. After cooling the mixture was extracted with dichloromethane (3×50 ml), filtered through celite, the solvent was evaporated and the residue crystallized from ethanol (50 ml) to give 3,3′,4,4′-tetrahexyloxybiphenyl (5.5 g, 50%) **4** as a white crystalline solid (mp 68–70 °C).[25] ^{1}H NMR ($CDCl_3$) δ: 7.13 (m, 4H, ArH), 6.90 (d, 2H, J=9 Hz, ArH), 3.97 (t, 8H, J=7 Hz, OCH_2), 1.81(m, 8H, J=7 Hz, OCH_2CH_2), 1.33–1.49(m, 24H, CH_2), 0.97 (t, 12H, J=7 Hz, CH_3).

1,2-Di(d_{13}-hexyloxy)benzene 5

Perdeuterated hexylbromide (560 mg; 3.39 mmol) **2**, catechol (170 mg; 1.54 mmol) **6** and anhydrous potassium carbonate (500 mg) were stirred in refluxing ethanol (20 ml) for 72 h. On completion, the mixture was decanted onto water (20 ml), extracted with dichloromethane (2×20 ml) and the solvent evaporated to give 1,2-di(d_{13}-hexyloxy)benzene **5** (313 mg; 67%) as a clear colorless liquid. ^{1}H NMR ($CDCl_3$) δ: 6.88 (s, 4H, ArH).

2,3-*Di(d_{13}-hexyloxy)-6,7,10,11-tetrahexyloxytriphenylene* 7

Anhydrous iron (III) chloride (680 mg) was added to a vigorously stirred solution of 1,2-di(d_{13}-hexyloxy)benzene (313 mg; 1.03 mmol) **5** and 3′,3,4′,4-tetrahexyloxybiphenyl (560 mg; 1.02 mmol) **4** in dry dichloromethane (25 ml). After 1 h the mixture was poured onto methanol (40 ml) and the resultant precipitate filtered-off. The crude residue was purified by column chromatography [silica, light petroleum: dichloromethane (1:1)] to give 2,3-di(d_{13}-hexyloxy)-6,7,10,11-tetrahexyloxytriphenylene (526 mg; 60%) **7** as a white solid. (K 69 °C D 99 °C I).[26] (Lit K-D 68 °C, D-I 99 °C). ^{1}H NMR ($CDCl_3$) δ: 7.83 (s, 6H, ArH), 4.23 (t, 8H, OCH_2), 1.94 (m, 8H, OCH_2CH_2), 1.41–1.56 (m, 24H, CH_2), 0.93 (t, 12H, CH_3).

Ring deuterated HAT6

2,3,6,7,10,11-Hexahexyloxy-1,4,5,8,9,12-hexadeuterotriphenylene

2,3,6,7,10,11-Hexahexyloxytriphenylene[27] (1 g; 1.2 mmol) and deuterated trifluoroacetic acid (1.1 ml) were stirred in deuterated chloroform (10 ml) for 72 h. On completion the mixture was poured carefully onto deuterated methanol (20 ml), cooled to 0 °C and the resulting precipitate filtered off to give 2,3,6,7,10,11-hexahexyloxy-1,4,5,8,9,12-hexadeuterotriphenylene (750 mg; 75%) as an off-white solid. (K 69.5 °C D 99.7 °C I). (Lit K-D 68 °C, D-I 99 °C). [M^+ (833)]. ^{1}H NMR ($CDCl_3$) δ: 7.83 (s, 1.5H, ArH), 4.23 (t, 12H, J=7 Hz, OCH_2), 1.94 (m, 12H, OCH_2CH_2), 1.41–1.56 (m, 36H, CH_2), 0.93 (t, 18H, J=7 Hz, CH_3).

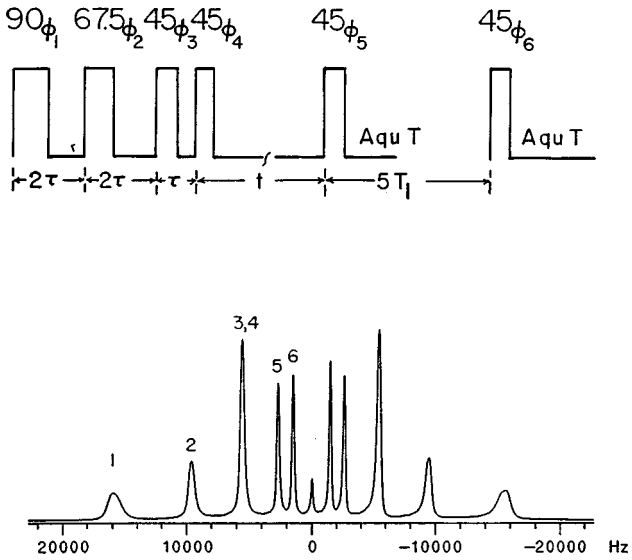

FIG. 2. A typical deuteron NMR spectrum of chain-deuterated HAT6 (the peak assignments are labeled by carbon numbers in the chain) and the modified broadband Jeener-Broekaert pulse sequence.

NMR

We determined the discotic-isotropic transition temperature T_c of our samples by means of NMR signals. The chain-deuterated sample exhibited a T_c=99.4 °C, while the ring-deuterated sample a T_c=100.4 °C. When comparing the NMR data of these samples, we scaled the temperatures to give a common T_c of 99.9 °C. The T_{1Z} and T_{1Q} of the methylene and ring deuterons were measured as a function of temperature at two Larmor frequencies. The HAT6 molecule is schematically shown in Figure 1 and the peak assignments for the chain-deuterated sample are shown on the representative spectrum in Figure 2. A home-built superheterodyne coherent pulse NMR spectrometer was operated for deuterons at 15.1 MHz using a varian 15 in electromagnet and at 46.05 MHz using a 7.1 Tesla Oxford superconducting magnet. The sample was placed in a NMR probe whose temperature was regulated either by an external oil bath circulator or by air flow with a Bruker BST-1000 controller. The temperature gradient across the sample was estimated to be better than 0.3 °C. The $\pi/2$ pulse width of about 3.8 μs was produced by a ENI power amplifier. Pulse control and signal collection were performed by a General Electric 1280 computer. Fourier transformation and data processing were completed by Spectral Calc and Micro Origin softwares on a IBM-PC computer. Broadband Jeener-Broekaert (J-B) excitation sequence (Figure 2) was used to simultaneously measure T_{1Z} and T_{1Q}. The data manipulation has been detailed elsewhere.[23] The pulse sequence was modified using an additional monitoring $\pi/4$ pulse to minimize any long-term instability of the spectrometer. This pulse was phase-cycled to have a net effect of subtracting the equilibrium magnetization (M_∞) signal from the J-B sequence. Signal collection was started 10 μs after each monitoring $\pi/4$ pulse, and averaged over 1024–4096 scans at 46 MHz and 2048–8192 scans at 15.1 MHz depending on the signal strengths of the

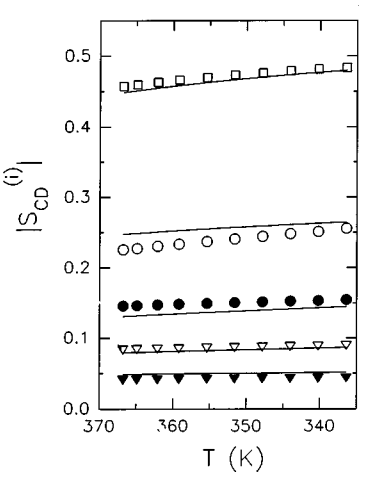

FIG. 3. Plots of segmental order parameters as a function of temperature in the columnar phase of HAT6. Square denotes the aromatic sites, open and closed circles denote C_1 and C_2, respectively, while open and closed triangles denote C_{3-4} and C_5, respectively. The solid curves are the theoretical predictions using the additive potential method.

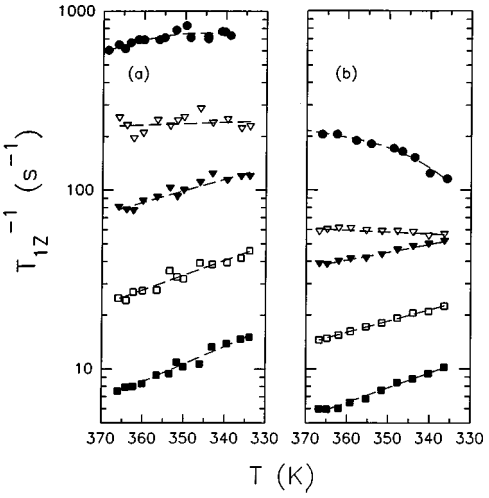

FIG. 4. Plot of experimental Zeeman spin-lattice relaxation rates versus the temperature in the columnar phase of HAT6. (a) and (b) are for data at 15.1 and 46 MHz, respectively. Circle denotes the aromatic sites, open and closed triangles denote C_1 and C_2, respectively, while open and closed squares denote C_{3-4} and C_5, respectively. The dashed lines are drawn to aid the eyes.

various resolvable peaks. For the spectrum with very small quadrupolar splittings, a larger value of pulse interval $\tau(\simeq 10\ \mu s)$ was required to maximize the quadrupolar order, comparing to the typical value of $\tau(5\mu\ s)$. Despite using broadband excitation of quadrupolar order, different sets of relaxation delays with appropriate repetition times were used. This was due to a large spread in the magnitude of the relaxation times for various deuterons. T_{1Z} and T_{1Q} were derived from a least-squares fit of the sum, $S(t)$, and difference, $D(t)$, of the component areas of the quadrupolar doublet:

$$S(t) \propto \exp(-t/T_{1Z}),$$

$$D(t) \propto \exp(-t/T_{1Q}).$$

The subtraction of the M_∞ signal in the pulse sequence meant that the above simple exponential equations could be used. The experimental uncertainty in these spin-lattice relaxation times was estimated to be $\pm 5\%$. The quadrupolar splittings of the aromatic site deuterons and chain deuterons were determined from NMR spectra obtained by Fourier transforming the free induction decay (FID) signal after a $\pi/2$ pulse, and had an experimental error of better than $\pm 1\%$. As seen in Figure 2, the doublet splittings from C_3 and C_4 sites are not resolved. Thus the spin-lattice relaxation times at these sites cannot be measured separately.

RESULTS AND DISCUSSION

Figure 3 shows the experimental $S_{CD}^{(i)}$ versus the temperature. The temperature dependencies of the measured relaxation rates T_{1Z}^{-1} and T_{1Q}^{-1} are summarized in Figures 4 and 5. The relaxation rates measured at 46 MHz are similar to those reported in the literature,[13] except our values for the aromatic deuterons are slightly lower and the values for the C_1 deuterons show slightly different temperature behaviors. In fitting the segmental order profiles, we had inputted various values of E_{tg}, E'_{tg}, $E_{g\pm g\mp}$, and $E'_{g\pm g\mp}$. We found that the calculated $\Delta\nu_3$ and $\Delta\nu_4$ were different and the best results were obtained by using $E_{tg}=3.7$ kJ/mol, $E'_{tg}=1.9$ kJ/mol, and $E_{g\pm g\mp}=E'_{g\pm g\mp}=10$ kJ/mol. The E_{tg} value is closed to the value used in the calamitic liquid crystal 6OCB,[23] but it is not clear why the E'_{tg} should be smaller than that used in 6OCB. An optimization routine[28] (AMOEBA) was used to minimize the sum squared error f in fitting the splittings

$$f=\sum_i (|S_{CD}^{(i)}|-|S_{CD}^{(i),calc}|)^2, \tag{22}$$

where the sum over i includes C_1 to C_5 and aromatic deuterons. The f values are of the order of 10^{-3} (see Table I). The calculated segmental order parameters are indicated in Figure 3 as solid lines. Note that $\Delta\nu_3$ and $\Delta\nu_4$ were aver-

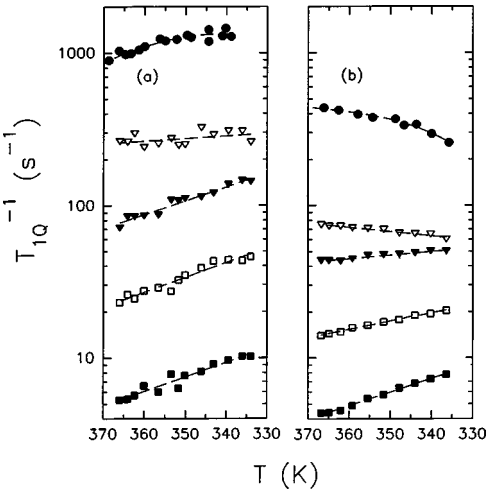

FIG. 5. Plot of experimental quadrupolar spin-lattice relaxation rates versus the temperature in the columnar phase of HAT6. (a) and (b) are for data at 15.1 and 46 MHz, respectively. Circle denotes the aromatic sites, open and closed triangles denote C_1 and C_2, respectively, while open and closed squares denote C_{3-4} and C_5, respectively. The dashed lines are drawn to aid the eyes.

TABLE I. Model parameters derived from the analysis of quadrupolar splittings at different temperatures in the columnar phase of HAT6. The interaction parameters X_a and X_{cc} are in units of kJ/mol. a_{20}, a_{22} are dimensionless second rank coefficients in the orienting potential which is used in the rotational diffusion equation.

T(K)	X_a	X_{cc}	$\langle P_2\rangle$	$\langle S_{xx}-S_{yy}\rangle$	a_{20}	$10^2 a_{22}$	$10^3 f$
364.9	17.3	0.145	0.848	0.00101	−7.0	−10.5	1.5
362.1	17.9	0.136	0.855	0.00087	−7.3	−10.0	1.5
359.2	18.5	0.124	0.862	0.00073	−7.6	−9.3	1.4
355.4	19.4	0.111	0.869	0.00059	−8.1	−8.4	1.4
351.6	20.4	0.098	0.878	0.00046	−8.6	−7.5	1.3
347.8	21.2	0.085	0.884	0.00037	−9.0	−6.6	1.3
344.0	22.2	0.072	0.890	0.00028	−9.5	−5.7	1.2
340.2	23.1	0.058	0.896	0.00021	−10.0	−4.7	1.2
336.4	24.1	0.050	0.902	0.00016	−10.6	−4.1	1.1

aged for comparison with the experimental values. We summarize in Table I some of the derived parameters $X_a, X_{cc}, \langle P_2\rangle, \langle S_{xx}-S_{yy}\rangle, a_{20}$ and a_{22}. As seen in Table I, $\langle S_{xx}-S_{yy}\rangle$ is vanishingly small indicating that the HAT6 molecule is essentially a uniaxial molecule.

The relations between the relaxation rates (measured with the director at 90° with the field direction) and the spectral densities as given by the general relaxation theory are

$$T_{1Q}^{-1} = 3J_1(\omega, 90°), \tag{23}$$

$$T_{1Z}^{-1} = J_1(\omega, 90°) + 4J_2(2\omega, 90°). \tag{24}$$

From the results of Figures 4–5 and the above equations, the spectral densities of the aromatic and aliphatic deuterons could be determined. These are summarized in Figures 6 and 7. To show the site dependence of spectral densities, we plot them in Figure 8 for two different temperatures. The $J_1(\omega, 90°)$ and $J_2(2\omega, 90°)$ are in general largest at the aromatic site ($i=0$) and decrease monotonically along the chain to the methyl group. At 336.4 K and 46 MHz, $J_2(2\omega, 90°)$ of C_0 is slightly less than that of C_1. We model the spectral densities by using Eqs. (18)–(21). In particular, we take advantage of the fact that the target parameters of the model vary smoothly with temperature by simultaneously analyzing data at all temperatures. From individual target analyses (i.e., analyze the data at each temperature), we found that the rotational diffusion constants and the jump constant k_2 obey simple Arrhenius-type relations, giving

$$D_\perp = D_\perp^0 \exp[-E_a^\perp/RT], \tag{25}$$

$$D_\parallel = D_\parallel^0 \exp[-E_a^\parallel/RT], \tag{26}$$

$$k_2 = k_2^0 \exp[-E_a^{k_2}/RT]. \tag{27}$$

In Eqs. (25)–(27), the global parameters are pre-exponentials $D_\perp^0$, $D_\parallel^0$, k_2^0, and their corresponding activation energies $E_a^\perp$, $E_a^\parallel$, $E_a^{k_2}$. For convenience, the diffusion and jump rate

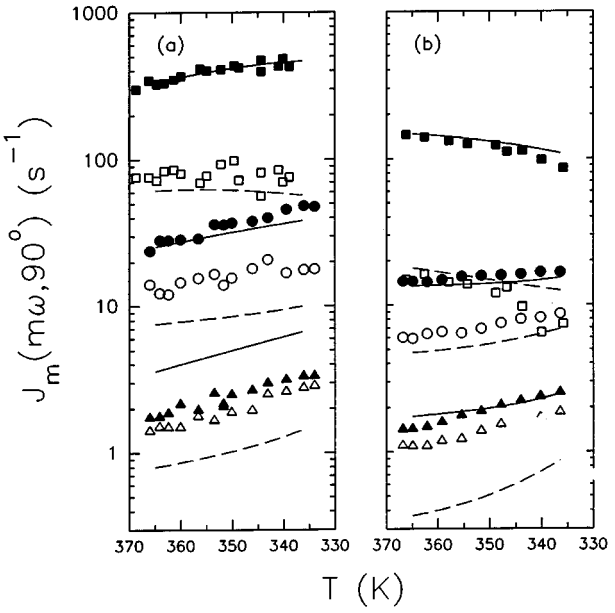

FIG. 6. Plots of experimental (symbols) and calculated (lines) spectral densities of HAT6. (a) and (b) are for data obtained at 15.1 and 46 MHz. The closed symbols denote $J_1(\omega_0, 90°)$, while the open symbols denote $J_2(2\omega_0, 90°)$. The triangles represent data for C_5, while the squares and circles represent data at the aromatic sites and C_2, respectively.

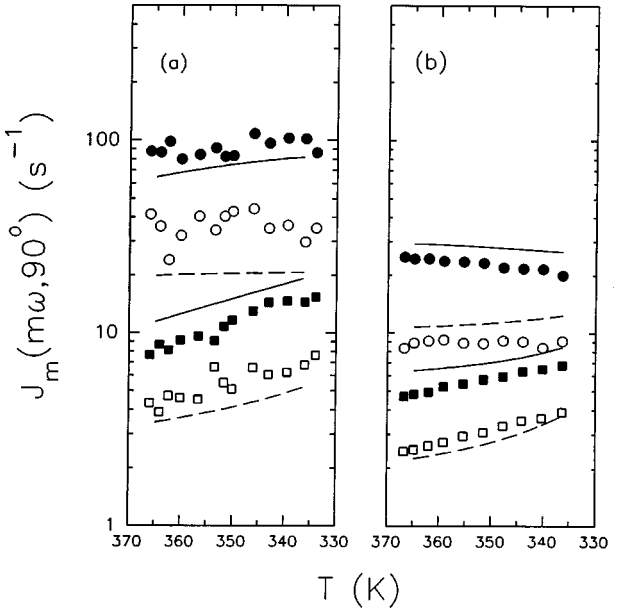

FIG. 7. Plots of experimental (symbols) and calculated (lines) spectral densities of HAT6. (a) and (b) are for data obtained at 15.1 and 46 MHz. The closed symbols denote $J_1(\omega_0, 90°)$, while the open symbols denote $J_2(2\omega_0, 90°)$. The circles represent data for C_1, while the squares represent data at C_{3-4}.

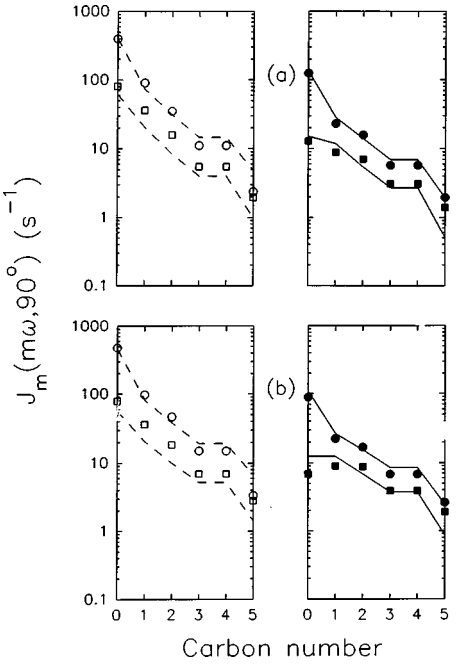

FIG. 8. Plots of spectral densities as a function of carbon position at (a) 351.6 K and (b) 336.4 K. Circle denotes $J_1(\omega_0,90°)$, and square denotes the corresponding $J_2(2\omega_0,90°)$. Open and closed symbols denote data at 15.1 and 46 MHz, respectively. The dashed and solid lines denote theoretical predictions at 15.1 and 46 MHz, respectively.

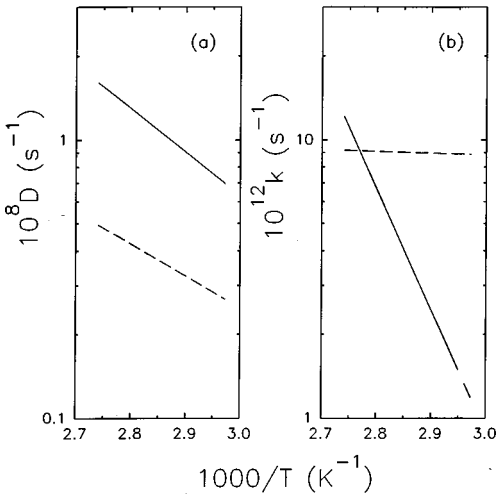

FIG. 9. Plots of (a) rotational diffusion constants and (b) jump constants as a function of the reciprocal temperature. Solid lines denote $D_\perp$ in (a) and k_2 in (b), while dashed lines denote $D_\parallel$ in (a) and k_3 in (b).

pre-exponentials are not used as global parameters. Rather Eqs. (25)–(27) are rewritten in terms of the activation energies and the diffusion and jump constants $D'_\perp$, $D'_\parallel$, k'_2 at $T_{max}=364.9$ K. When such a relation does not exist for a target parameter like k_1 or k_3, it is still possible to introduce an interpolating relation linking its values at various temperatures. As k_1 and k_3 are weakly temperature dependent, we model them by a linear relation:

$$k_i = k'_i - k''_i(T - T_{max}), \tag{28}$$

where the global parameters k'_i, and $k''_i (i=1$ or 3) are optimized. The diffusion constants $D'_\perp$, $D'_\parallel$ and the jump constants k'_1, k'_2, k'_3 at T_{max} were first obtained from an individual target analysis. Again AMOEBA was used in our minimization to fit the spectral density data. The sum squared percent error F is given by

$$F = \sum_k \sum_\omega \sum_i \sum_m \left[\frac{J_m^{(i)calc}(m\omega,90°) - J_m^{(i)}(m\omega,90°)}{J_m^{(i)}(m\omega,90°)} \times 100 \right]_k^2, \tag{29}$$

where the sum over k is for nine temperatures, ω for two frequencies, i for five methylene deuterons (and aromatic deuterons) and $m=1$ or 2. The fitting quality factor Q is given by the percent mean-squared deviation

$$Q = \frac{\Sigma_k \Sigma_\omega \Sigma_i \Sigma_m [J_m^{(i)calc}(m\omega,90°) - J_m^{(i)}(m\omega,90°)]_k^2}{\Sigma_k \Sigma_\omega \Sigma_i \Sigma_m [J_m^{(i)}(m\omega,90°)]_k^2} \times 100. \tag{30}$$

Again the calculated spectral densities for C_3 and C_4 are quite different. However, we have averaged the calculated spectral densities at these two sites in our minimization. Because the ring $J_1(\omega,90°)$ is larger than all the other spectral densities, we have adopted the strategy to first minimize the sum squared error (i.e., Q). As the global fit appeared to be insensitive to the $E_a^\perp$ value, we have chosen to derive nine global parameters from a total of 432 spectral densities with several input $E_a^\perp$ values. There was hardly any change in the Q value when varying $E_a^\perp$ between 10 and 30 kJ/mol. Thus we have chosen the value $E_a^\perp = 30$ kJ/mol, simply because it was slightly larger than the derived $E_a^\parallel$ of 22.0 $\pm$0.6 kJ/mol. By minimizing Q, a better fit of the ring data was achieved. We then used the derived motional parameters for the molecular reorientation, and minimized F using only the methylene data to get the jump constants. We summarize the rotational diffusion constants in Figure 9a. It is interesting to note from this figure that the rotational diffusion constant $D_\perp$ is larger than $D_\parallel$ in the entire columnar phase of HAT6. This is quite different from calamitic liquid crystals in which the spinning motion is much faster than the tumbling motion. The jump constant k_1 is essentially independent of the temperature ($k_1 = 5\times10^{17}\ s^{-1}$) and describes the fast one-bond motion of the last C–C bond in the chain. The k_2 and k_3 are given as a function of temperature in Figure 9b. As seen in the figure, k_3 decreases very slightly with decreasing temperature. Although jump constants have been obtained in several calamitic liquid crystals,[8] it is difficult at present to make comparison among them or with those obtained here. The activation energy for the two-bond motion is $E_a^{k_2} = 83.6$ kJ/mole. Its error limits range between 39 kJ/mol (for 13% increase in F) to 88.7 kJ/mol. The error limit for a particular global parameter was estimated by varying the one under consideration while keeping all other global parameters identical to those used for the minimum F (or Q), to give an approximate doubling in the Q value (e.g., $E_a^\parallel$) or in the F value (e.g., $k'_1, E_a^{k_2}$). When the target parameter becomes insensitive in the calculation, a lower % increase in F was

used. Now the pre-exponentials in Eqs. (25)–(27) are $D_{\parallel}^{0}=7.05\times10^{10}\ \mathrm{s}^{-1}$, $D_{\perp}^{0}=3.17\times10^{12}\ \mathrm{s}^{-1}$, and $k_2^0=1.1\times10^{25}\ \mathrm{s}^{-1}$. The uncertainty in $D_{\parallel}^{0}$ is $5.6–8.5\times10^{10}\ \mathrm{s}^{-1}$ and in $D_{\perp}^{0}$ is between $5\times10^{11}\ \mathrm{s}^{-1}$ and $1.1\times10^{13}\ \mathrm{s}^{-1}$. We note that at the low $D_{\perp}^{0}$ limit, the $D_{\parallel}/D_{\perp}$ ratio is about 2. The error limits for k_2^0 are between $1.9\times10^{24}\ \mathrm{s}^{-1}$ and $1\times10^{28}\ \mathrm{s}^{-1}$ (for 13% increase in F). At T_{max}, $k_1'=5.0\times10^{17}\ \mathrm{s}^{-1}$ and $k_3'=9.19\times10^{12}\ \mathrm{s}^{-1}$. The error bar for k_3' ranges between $4.25\times10^{12}\ \mathrm{s}^{-1}$ to $2.4\times10^{14}\ \mathrm{s}^{-1}$. While any larger k_1' value does not affect the fit, its lower limit is found to be $2\times10^{12}\ \mathrm{s}^{-1}$. Finally, the calculated spectral densities for HAT6 ($Q=0.67\%$) are indicated by curves in Figures 6 and 7. Although the final Q value is quite small, there exist large systematic deviations between the calculated and experimental spectral densities at some carbon sites (e.g., C_5). We attribute these discrepancies to the limitation and assumptions in the model used in the present study. The predicted site dependencies of various spectral densities at two temperatures are also shown in Figure 8.

In conclusion, we have given a consistent interpretation of both the quadrupolar splittings and the spin-lattice relaxation data measured in the columnar phase of two differently deuterated HAT6 molecules. From modeling the splittings with the AP method, we obtain the orienting potential needed to describe the reorientational dynamics of molecular disks. It is clear that the tumbling motion of a disk can be slightly faster than its spinning motion. Given the rotational diffusion constants are of the order of $10^8\ \mathrm{s}^{-1}$, the packing of molecular disks within a column must be viewed as a state of high dynamic mobility. The decoupled model proposed by Dong[18] for correlated internal rotations has been applied for the first time to a discotic liquid crystal.

Finally, we comment on the very interesting implications of the results for electronic transport along the molecular columns. The rotational speeds $D_{\parallel}$ and $D_{\perp}$ are some two orders of magnitude slower than a typical charge hopping frequency ($10^{10}\ \mathrm{s}^{-1}$) between the aromatic cores of adjacent molecules. The implication is that on the time scale of charge diffusion the ''lattice'' appears static with disorder being due to instantaneous displacement of HAT6 molecules with respect to each other. This dynamically induced disorder has consequences both in the quantum (low temperatures) and the stochastic hopping (high temperatures) limits. In the quantum limit, the disorder will cause elastic scattering and reduce the charge mobility. In the stochastic hopping limit it produces variations in jump frequencies between adjacent molecules in the columns. This, in turn, gives rise to a frequency dependent diffusivity.

ACKNOWLEDGMENTS

The financial support of the Natural Sciences and Engineering Council of Canada and the technical assistance of N. Finlay are gratefully acknowledged. We also acknowledge the Engineering and Physical Sciences Research Council of Great Britain for the award of research studentships to A.W. and P.S.M., and Dr. B. Movaghar for helpful discussion on the mechanism of charge transport in discotic liquid crystals. R.Y.D. also acknowledges a travel grant from the Association of Universities and Colleges of Canada.

[1] S. Chandrasekhar and G. S. Raganath, Rep. Prog. Phys. **53**, 57 (1990).
[2] N. Boden, R. Bissell, J. Clements, and B. Movaghar, Curr. Sci. **71**, 599 (1996).
[3] D. Adam, F. Closs, T. Frey, D. Funhoff, D. Haarer, H. Ringsdorf, P. Schumacher, and S. K. Siemensmeyer, Phys. Rev. Lett. **70**, 457 (1993).
[4] D. Adam, P. Schumacher, J. Simmeree, K. H. Etzbach, H. Ringsdorf, and D. Haarer, Nature (London) **371**, 142 (1994).
[5] N. Boden, R. J. Bushby, J. Clements, B. Movaghar, K. Donovan, and T. Kreouzis, Phys. Rev. B **52**, 13274 (1995).
[6] N. Boden, R. J. Bushby, and J. Clements, J. Chem. Phys. **98**, 5920 (1993).
[7] R. Y. Dong, D. Goldfarb, M. Moseley, Z. Luz, and H. Zimmermann, J. Phys. Chem **88**, 3148 (1984).
[8] R. Y. Dong, *Nuclear Magnetic Resonance of Liquid Crystals*, 2nd ed. (Springer-Verlag, New York, 1997).
[9] P. L. Nordio and P. Busolin, J. Chem. Phys. **55**, 5485 (1971); P. L. Nordio, G. Rigatti, and U. Segre, J. Chem. Phys. **56**, 2117 (1972).
[10] R. Tarroni and C. Zannoni, J. Chem. Phys. **95**, 4550 (1991).
[11] D. Goldfarb, Z. Luz, and H. Zimmermann, J. Phys. (Paris), Colloq. **42**, 1303 (1981).
[12] D. Goldfarb, Z. Luz, and H. Zimmermann, J. Chem. Phys. **78**, 7065 (1983).
[13] D. Goldfarb, R. Y. Dong, Z. Luz, and H. Zimmermann, Mol. Phys. **54**, 1185 (1985).
[14] G. M. Richards and R. Y. Dong, Liq. Cryst. **5**, 1011 (1989).
[15] G. Q. Cheng and R. Y. Dong, J. Chem. Phys. **89**, 3308 (1988).
[16] S. Marcelja, J. Chem. Phys. **60**, 3599 (1974).
[17] J. W. Emsley, G. R. Luckhurst, and C. P. Stockley, Proc. R. Soc. London, Ser. A **381**, 117 (1982).
[18] R. Y. Dong, Phys. Rev. A **43**, 4310 (1991).
[19] P. J. Flory, *Statistical Mechanics of Chain Molecules* (Interscience, New York, 1969).
[20] R. Y. Dong, Mol. Phys. **88**, 979 (1996).
[21] G. R. Luckhurst, C. Zannoni, P. L. Nordio, and U. Segre, Mol. Phys. **30**, 1345 (1975).
[22] C. J. R. Counsell, J. W. Emsley, N. J. Heaton, and G. R. Luckhurst, Mol. Phys. **54**, 847 (1985).
[23] C. J. R. Counsell, Ph.D. thesis, Southampton (1983); C. J. R. Counsell, J. W. Emsley, G. R. Luckhurst, and H. S. Sachdev, Mol. Phys. **63**, 33 (1988).
[24] R. Y. Dong, L. Friesen, and G. M. Richards, Mol. Phys. **81**, 1017 (1994).
[25] N. Boden, R. C. Borner, R. J. Bushby, and A. N. Cammidge, UK Pat. Appl. 9312091.3, 11th June 1993.
[26] For a review of Ullmann coupling reactions see M. Goshaev, O. S. Otroschenka, and A. A. Sadykov, Russ. Chem. Rev. **41**, 12 (1972).
[27] N. Boden, R. C. Borner, R. J. Bushby, A. N. Cammidge, and M. V. Jesudason, Liq. Cryst. **15**, 851 (1993).
[28] W. H. Press, B. P. Flannery, S. A. Teukolsky, and W. T. Vetterling, *Numerical Recipes* (Cambridge University Press, Cambridge, 1986).